GEOPHYSICAL RESEARCH LETTERS, VOL. 24, NO. 23, PAGES 2965-2968, DECEMBER 1, 1997

Is the geoeffectiveness of the 6 January 1997 CME predictable from solar observations?

X. P. Zhao and J. T. Hoeksema

W.W. Hansen Experimental Physics Laboratory, Stanford University, Stanford, California

Abstract. We present a prediction scheme for specifying the duration and maximum strength of the southward IMF within a magnetic cloud from observations of the disappearing filament associated with the coronal mass ejection and the photospheric magnetic field made near the filament disappearing. Using this scheme we were able to predict that the Earth directed 6 January 1997 coronal mass ejection would be geoeffective. We expected that the southward IMF interval would have a maximum strength of -13 ± 5 nT and a duration of 14 ± 5 hours. This compares favorably with the WIND observations of -15 nT and 13 hours.

1. Introduction

The 6 January 1997 coronal mass ejection (CME) is well known for its heliospheric and terrestrial effects, unusual during solar minimum. This Sun-Earth connection event was observed by an impressive array of instruments on the SOHO and WIND spacecraft; such a comprehensive complement has never before.

The CME was observed by SOHO-LASCO coronagraphs at ~16 UT on 6 January and is assumed to be associated with a disappearing solar filament (DSF) that took place between 13 and 15 UT on 6 January. The DSF was located over the northern fringe of Region SN84, a large weak plage area with no sunspots near central meridian at S30. Radio and X-ray data on 6 January also show weak coronal activity associated with the DSF [*D. Webb*, private communication, 1997].

The halo shape of the CME and the associated coronal activity near disk center on the Earthward-facing side suggested that a magnetized ejector had originated near Sun's disk center and was heading toward the Earth. Indeed, a shock was observed by the WIND spacecraft near 1 AU at 01 UT on 10 January and a magnetic cloud passed the spacecraft between 05 UT on 10 January and 04 UT on 11 January. The cloud contained continuous southward interplanetary magnetic field (IMF) for 13 hours with a maximum hourly-averaged value of -15 nT [*Len Burlaga*, private communication, 1997].

The long-duration southward IMF triggered a geomagnetic storm at about 06 UT on 10 January. Eleven hours after the magnetic storm began, the GOES-9 alert threshold for dangerous levels of energetic electrons accelerated by the disturbed field was crossed.

The arrival of the ejector at the Earth on 10 January was successfully predicted by assuming a constant propagation velocity of 450 km/s [*Don Michels*, private communication, 1997]. It is well known that not all magnetized ejecta encountering the Earth's magnetosphere are geoeffective and even fewer cause any damage. Can we predict whether or not a CME will be geoeffective from solar observations? It has long been desired to answer the question, but few attempts have been successful.

We develop in Section 2 a prediction scheme for specifying the duration and maximum hourly-averaged value of the southward IMF within magnetic clouds from the orientation of the associated DSF's central axial field. In Section 3 we attempt to determine the geoeffectiveness of the 6 January 1997 CME-associated DSF using SOHO-MDI observations of the photospheric magnetic field made simultaneously with the 6 January CME-associated DSF. Finally we discuss how to improve the prediction scheme.

2. Prediction scheme

2.1. Prediction of magnetic cloud B_s events

It is now believed that the immediate cause of geomagnetic storms is long intervals of intense southward IMF, or B_s events, and that continuous intense southward IMF usually occurs within magnetic clouds [*Burlaga et al.*, 1981; *Tsurutani et al.*, 1992; *Zhao et al.*, 1993; *Bothmer and Schwenn*, 1994]. To distinguish B_s events that occur within magnetic clouds from those that occur within shock sheathes or are associated with large-amplitude Alfvenic fluctuations [*Tsurutani and Gonzalez,* 1997], we specifically call the former "magnetic cloud B_s events" in what follows. We define the maximum southward IMF field strength averaged over 1 hour in a magnetic cloud B_s event as the intensity of the B_s event. Interplanetary magnetic clouds have been associated with solar CMEs [*Gosling*, 1990 and references therein]. To predict whether or not a CME will be geoeffective, we need information about the internal magnetic field in the associated magnetic cloud and its solar counterpart as well as its propagation trajectory.

Paper number 97GL03000.
0094-8534/97/97GL-03000$05.00

The variations of magnetic field direction associated with the motion of a magnetic cloud past a spacecraft can be explained by a cylindrically symmetric force-free magnetic field configuration. The cylindrical rope field may be described in terms of two components that depend on the radial distance from its central axis alone, the axial and transverse components. The two components both depend on the central axial field vector, $\mathbf{B}_{ax}$ [*Burlaga* 1995 and references therein].

Based on the characteristics of 26 magnetic clouds determined using cylindrical magnetic flux rope models [*Lepping et al.*, 1990; *Marubashi*, 1997], we found that magnetic cloud $\mathbf{B}_{ax}$ orientations are evenly distributed between ecliptic latitudes of S90 and N90 degrees, and that their longitudinal occurrence frequency peaks slightly in the east and west [*Zhao and Hoeksema*, 1997]. Therefore, the southward field within a magnetic cloud will depend on not only the cloud's transverse component, but also on its axial component. In other words, the duration and intensity of a magnetic cloud B_s event depend on the direction and strength of the cloud's $\mathbf{B}_{ax}$. In addition, they also depend upon the size of the cloud, the interaction between the cloud and the solar wind, and the impact distance (the distance of the spacecraft near the Earth from the rope axis at closest approach point). As shown in what follows, the orientation of the cloud's $\mathbf{B}_{ax}$ and the impact distance are the only two quantities that may be estimated using solar observational data currently available. For most of the 14 events that we were able to use to establish the relationship between magnetic clouds and DSFs, the impact distance was less than 0.3 of the cloud radius. Here we analyze the dependence of the duration and intensity of magnetic cloud B_s events on the orientation of the cloud's $\mathbf{B}_{ax}$ only.

Using the OMNI hourly-averaged IMF data, the intensity and duration of magnetic cloud B_s events may be determined for 23 of the 26 magnetic clouds mentioned above; 3 clouds with a large data gap in their southward IMF interval are excluded. In the case of no southward IMF, the duration is defined as zero and the intensity as the smallest northward field strength.

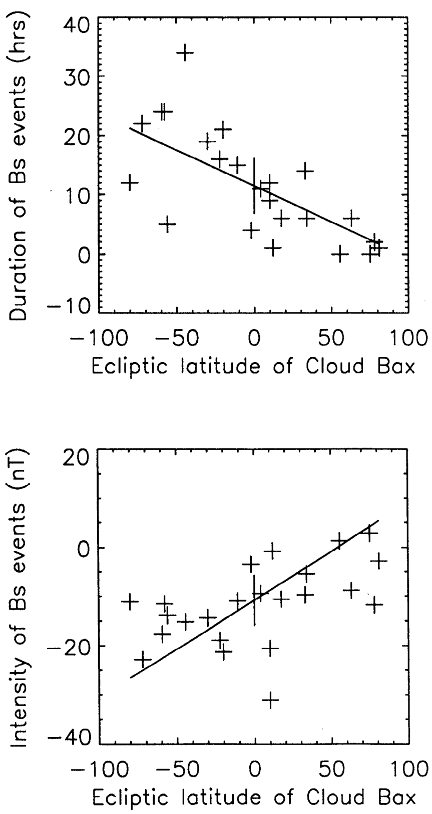

Figure 1. The dependence of the duration and intensity of magnetic cloud B_s events on the ecliptic latitude of the central axial field direction in magnetic clouds.

Figure 1 shows the regression relation between the characteristics of magnetic cloud B_s events and the ecliptic latitude of cloud's $\mathbf{B}_{ax}$. The linear dependence of the duration (D in hours) and intensity (I in nT) of a magnetic cloud B_s event on the ecliptic latitude (L_E in degrees) determined using a least square fitting technique are given by:

$$D = (11.49 - 0.12\, L_E) \pm 4.70 \qquad (1)$$

$$I = (-10.76 + 0.10\, L_E) \pm 5.12 \qquad (2)$$

2.2. Prediction of the orientation of magnetic clouds

Magnetic clouds have also been associated with DSFs, or eruptive prominences on the limb. Eruptive prominences and CMEs often occur together in a three-part structure: a bright outer rim located above a low density cavity that contains the prominence. Many believe that the interplanetary magnetic cloud corresponds to the central cavity because of its low β. It has been suggested recently that the observed bright rim-cavity-prominence features are three parts of one magnetically organized flux rope. In fact, the prominence gas is also a low-β structure because of the low temperature [*Chen*, 1997 and references therein].

Eruptive prominences often exhibit helical structures, suggestive of underlying magnetic fields with twisted field lines, such as magnetic flux rope. The magnetic fields in quiet filaments have been found to be preferentially sinistral heliform in the southern hemisphere and dextral in the northern hemisphere, regardless of solar cycle [*Martin et al.*, 1994]. This clear distinction of quiet filament field helicity by hemisphere has been confirmed in the field configuration observed in magnetic clouds [*Rust*, 1994; *Bothmer and Schwenn*, 1995; *Marubashi*, 1997].

Solar filaments are assumed to be basically parallel to the solar surface and observed in their projection against the chromosphere. The orientation of the DSF's $\mathbf{B}_{ax}$ may be expressed in terms of the angle from the local east-west line. Among the aforementioned 26 mag-

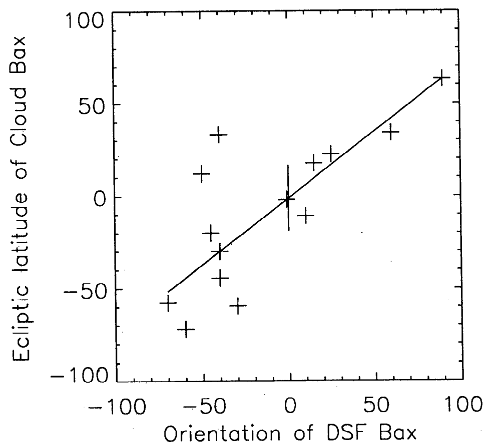

Figure 2. The dependence of the ecliptic latitude of of magnetic cloud central axial field direction on the orientation of DSF central axial field direction.

netic clouds, 14 clouds have been associated with DSFs (see Tables in Marubashi [1997] and Rust [1994]). By using UAG reports on disappearing filaments [*McIntosh*, 1979; *Wright*, 1991] and the appropriate photospheric field polarity data, the orientation of the 14 DSF's $\mathbf{B}_{ax}$ may be estimated using Martin's rule for handedness of filament field rotation.

Figure 2 displays the regression relations of the ecliptic latitude (L_E in degrees) of the direction of an interplanetary magnetic cloud's $\mathbf{B}_{ax}$ to the orientation (Fo in degrees) of the associated solar DSF's $\mathbf{B}_{ax}$

$$L_E = (-1.4 + 0.7\,Fo) \pm 17.8. \qquad (3)$$

The central axial field direction in the magnetic cloud and the associated DSF changes only slightly, though expansion and interaction of ejecta with the solar wind are expected to occur as it propagates through the interplanetary medium.

3. Prediction of the 10 January magnetic cloud B_s event

Section 2 indicates that the orientation of an interplanetary magnetic cloud's $\mathbf{B}_{ax}$ is determined by the orientation of $\mathbf{B}_{ax}$ in the associated DSF, and that the duration and intensity of a magnetic cloud B_s event depend on the cloud's $\mathbf{B}_{ax}$ for those clouds with a small impact distance.

The field configuration of the 6 January DSF is sinistral heliform according to Martin's handedness rule. To determine the orientation of the DSF's $\mathbf{B}_{ax}$ we need the field polarity distribution around the DSF at the time when the quiet filament disappeared. The 96-minute cadence SOHO/MDI observations of the photospheric magnetic field make it possible [*Scherrer et al.*, 1995].

Figure 3 displays the line-of-sight flux contours of the large-scale photospheric magnetic field at 12:48 UT on 6 January, just before the DSF took place. The plot is obtained by smoothing the MDI magnetic images from 1024 x 1024 to 64 x 64. The thick contours indicate polarity inversion lines where the line-of-sight field is zero. The polarity inversion line indicated by an arrow head is nearly colocated with the "radio filament" in the Nobeyama 17 GHz image at 06:45 on 6 January and is consistent with the location of the H_α filament [*D. Webb*, private communication, 1997].

The 6 January CME-associated DSF consists of two segments. One extended from S24W01 to S23W03 and the other from S24W01 to S27W00. In estimating the orientation of DSF's $\mathbf{B}_{ax}$, it is necessary to find the orientation of the associated polarity inversion line as well as the orientation of the DSF itself. Because both the orientation of the associated polarity inversion line and that of the "radio filament" are parallel to the the first segment, we use the orientation of the first segment to determine the orientation of the DSF's $\mathbf{B}_{ax}$. Using the 12:48 UT polarity distribution of the photospheric magnetic field around the sinistral heliform DSF, we determine that the orientation of the DSF's $\mathbf{B}_{ax}$ is -2… degrees. The ecliptic latitude of the 10 January magnetic cloud's $\mathbf{B}_{ax}$ is thus expected to be -20 degrees from Eq. (3), and the anticipated intensity and duration of the 10 January magnetic cloud B_s event may be determined from Eqs. (1) and (2) to be $-13 \pm$ … nT and 14 ± 5 hours, agreeing with WIND observations mentioned in Section 1.

4. Discussion

Whether or not a CME will be geoeffective depends on whether or not it encounters the Earth and generates a B_s event. The halo shape of the 6 January CME and the location of the associated DSF near the disk central

Figure 3. The line-of-sight flux contours of the large scale photospheric magnetic field measured at 12.48 UT on 6 January 1997 by the SOHO/MDI instrument. The solid and dotted lines denote positive and negative polarities, respectively. The thick lines are the polarity inversion lines. The associated DSF took place at 13:0… UT near the polarity inversion line indicated by an arrow.

meridian suggested that the ejector would encounter the Earth.

The prediction scheme developed here indicates that the orientation of the CME-associated DSFs' $\mathbf{B}_{ax}$ relative to the Earth's magnetic field determines the degree of geoeffectiveness by way of the duration and intensity of magnetic cloud B_s events. The simultaneous observations of the CME-associated DSF and the polarity distribution of the photospheric magnetic field are needed to estimate the orientation of the CME-associated DSF's $\mathbf{B}_{ax}$. The specified duration and intensity for the 10 January magnetic cloud B_s event agree quite well with the observations of the WIND spacecraft.

In addition to the orientation of the CME-associated DSF's central axial field as the input to the prediction scheme developed here, the impact distance is another important factor that affects the characteristics of magnetic cloud B_s events near the Earth and that can be estimated using solar observational data currently available. Because the impact distances for most of the magnetic clouds used to produce Figure 2 are small, as mentioned in Section 2, the prediction scheme here is valid only for those CME-associated DSFs that occur near the solar disk center, like the 6 January DSF. Using a larger CME-associated DSF data set with a greater range of impact distances, the dependence of magnetic cloud B_s events on the impact distance and the relationship between the impact distance and the location of the CME-associated DSF on the solar disk may be studied, and the prediction scheme may be improved by using a multiple regression analysis.

It should be noted that the standard deviation in the scheme is not small. The prediction scheme may be further improved by considering the propagation speed of ejecta. One must need measure (or infer) the propagation speed of CMEs in the line-of-sight direction and develop a magnetic cloud model that includes the interaction between ejecta and the solar wind. The measurement of the central axial field in filaments is also needed to predict the strength of magnetic clouds' $\mathbf{B}_{ax}$. There is a long way to go to improve the prediction scheme developed here.

Acknowledgments. We thank K. Marubashi for providing us his useful preprint. This work was supported by the National Aeronautics and Space Administration under Grants NAGW 2502 and NAG5-3077, by the Atmospheric Sciences Section of the National Science Foundation under Grant ATM9400298, and by the Office of Naval Research under Grants N00014-89-J-1024 and N0014-97-1-0129. The MDI development was supported by NASA contract NAS5-30386 at Stanford University.

References

Bothmer, V. and R. Schwenn, Eruptive prominences as sources of magnetic clouds in the solar wind, in *Mass Supply and Flows in the Solar Corona,* edited by B. Fleck, G. Noci and G. Polleto, p. 215, Kluwer, Norwell, MA, 1994.

Bothmer, V. and R. Schwenn, The interplanetary and solar causes of major magnetic storms, *J. Geomag. Geoelectr., 47,* 1127, 1995.

Burlaga, L. F., *Interplanetary Magnetohydrodynamics*, Oxford University Press, New York, 1995.

Burlaga, L. F., E. Sittler, F. Mariani, and R. Schwenn, Magnetic loop behind an interplanetary shock: Voyager, Helios and IMP-8 observations, *J. Geophys. Res., 86,* 6673, 1981.

Chen, J., Prominence eruptions and geoeffective solar wind structures, in *Magnetic Storms, Geophys. Monogr. Ser.*, Vol. 98, edited by B. T. Tsurutani et al., p. 45, AGU, Washington DC, 1997.

Gosling, J. T., Coronal mass ejections and magnetic flux ropes in interplanetary space, in *Physics of Magnetic Flux Ropes, Geophys. Monogr. Ser.,* Vol. 58, edited by C. T. Russell, E. R. Priest, and L. C. Lee, p. 343, AGU, Washington DC, 1990.

Lepping, R. P., J. A. Jones, and L. F. Burlaga, Magnetic cloud structure of interplanetary magnetic clouds at 1 AU, J. Geophys. Res., *95,* 11957–11965, 1990.

Martin, S. F., R. Bilimoria, and P. W. Tracadas, Magnetic field configurations basic to filament channels and filaments, in *Solar Surface Magnetism,* edited by R. J. Rutten and C. J. Schrijver, pp. 308–338, Kluwer, 1994.

Marubashi, K., Interplanetary magnetic flux ropes and solar filaments, in *Coronal Mass Ejections, Geophys. Monogr. Ser.*, Vol. 99, edited by N. Crooker et al., p. 147, AGU, Washington DC, 1997.

McIntosh, P. S., Annotated atlas of H_α synoptic charts for Solar Cycle 20 (1964–1974), *Report UAG-70,* World Data Center A Solar Terrestrial Physics, NOAA, Boulder, 1979.

Rust, D. M., Spawning and shedding helical magnetic fields in the solar atmosphere, Geophys. Res. Lett., *21,* 241-244, 1994.

Scherrer, P. H., et al., The solar oscillations investigation – Michelson doppler imager, *Solar Phys., 162,* 129, 1995.

Tsurutani, B. T. and W. D. Gonzalez, The interplanetary causes of magnetic storms: A review, in *Magnetic Storms, Geophys. Monogr. Ser.*, Vol. 98, edited by B. T. Tsurutani et al., p. 77, AGU, Washington DC, 1997.

Tsurutani, B. T., W. D. Gonzalez, F. Tang, and Y. T. Lee, Great magnetic storms, Geophys. Res. Lett., *19,* 73-76, 1992.

Wright, C. S., Catalog of solar filament disappearances 1964–1980, *Report UAG-100,* World Data Center A Solar Terrestrial physics, NOAA, Boulder, 1991.

Zhao, X. P., J. T. Hoeksema, J. T. Gosling, and J. L. Phillips, Statistics of IMF Bz events, in *Solar-Terrestrial Predictions Workshop-IV,* edited by J. Hruska et al., pp. 712–719, Natl. Oceanic and Atmospheric Administration, Boulder, Vol. 2, 1993.

Zhao, X. P. and J. T. Hoeksema, The central axial field direction in magnetic clouds and its relation to southward IMF events and dependence on disappearing solar filaments, J. Geophys. Res., , in press, 1997.

X. P. Zhao and J. T. Hoeksema, Stanford University, HEPL Annex B, Stanford, CA 94305-4085. (e-mail: xpzhao@solar.stanford.edu; jhoeksema@solar.stanford.edu)

(Received April 30, 1997; revised July 25, 1997; accepted October 15, 1997.)